This is a peer-reviewed, accepted author manuscript of the following conference paper: Gebremedhin, T, Xu, L, Chen, Y & Chen, D 2025, Assessment of interactions of multiple converters and network considering impedance change. in 2024 IEEE PES Innovative Smart Grid Technologies Europe (ISGT EUROPE). IEEE, Piscataway, NJ. https://doi.org/10.1109/isgteurope62998.2024.10863807

Assessment of Interactions of Multiple Converters and Network Considering Impedance Change

Tesfu Gebremedhin[1]
Department of Electrical and electrons Engineering
University of Strathclyde, Glasgow, UK
Tesfu.gebremedhin.2016@strath..uk

Lie Xu[1]
Department of Electrical and Electrons Engineering
University of Strathclyde, Glasgow, UK
email: lie.xu@strath.ac.uk

Yin Chen[1]
Department of Electrical and electrons Engineering
University of Strathclyde, Glasgow, UK
email: Yin.chen101@strath.ac.uk

Dong Chen[2]
UK National HVDC Centre
Scotland, Glasgow, UK
email: Dong.Chen@sse.com

***Abstract*-This paper addresses the stability challenges arising from the integration of multiple converters into an AC network, spotlighting on potential instabilities generated by the interplay between converter control loops and the network's passive components. Employing an impedance-based approach that incorporates impedance ratio (IR) and examining a different control configuration such as active and reactive Power (PQ) and active Power and AC voltage (PV), alongside other parameters like phase-Locked loop (PLL), this work examines methodically the dynamic interactions. Through IR, it evaluates the individual impacts of converter (remote converter) on network equivalents, thereby elucidating how the interaction between converters and the broader network influences overall system stability. Ultimately, the proposed methodology aids in identifying impedance variations and potential instabilities in grid-tied converters, offering a roadmap for the perceptive design of converters and network parameter configurations.**

Keywords: **Converter Impedance, Eigenvalue Analysis, Impedance Ratio (IR), Impedance-Method Approach, Multi-Voltage Source Converter, Network Impedance, Phase-Locked Loop (PLL).**

1. INTRODUCTION

In the modern era, power electronic converters have been widely used in modern power systems for transmitting power generated by renewable and clean energy sources to the grid system [1][2]. Nonetheless, potential interactions between the control loops of these converters and the passive elements of the network may give rise to instability issues [3][4]. The impedance method, examining the dynamic interplay between converters and networks [5]– [8], presents a formidable avenue for stability assessment. The development of efficient methods for evaluating impedance-type stability in multiple converter systems is a key goal, promising enhancements in system stabilities.

Impedance-based methodologies elucidate the complex influences on converter stability, highlighting the crucial functions of converter control dynamics and digital system time delays in fostering negative resistive behaviours that could lead to resonance destabilization [3]. Recent findings spotlight Phase-Lock Loop (PLL) complexities in grid-connected converters under weak grid scenarios, revealing how PLL-induced impedances might act as negative incremental resistors, influenced by PLL bandwidth and converter power [5][6]. Additionally, the impact of grid input impedance, injection currents, and reactive components on converter

performance underscores the intricacies of grid-connected operations. These stability challenges are exacerbated in multi-converter systems, propelling network impedance analysis to the forefront of research, with numerous investigations aiming to dissect and address these concerns, thereby enhancing overall system stability [7][8][9].

Extensive research has been dedicated to multi-converter stability in power systems, utilizing state-space or impedance models. Integrating numerous distributed generations complicates the state-space approach, making stability assessments laborious [10]. However, utilizing integrated and sparse impedance models simplifies this process [11][12]. Identifying key converters causing instability enhances multi-converter system stability, offering direction for controller parameter adjustments and promoting effective design strategies.

This paper investigates a methodology considering impedance ratio (IR) change and eigenvalue analysis to clarify the intricate dynamics of multi-converter interactions. Specifically, it aims to identify specific frequencies where impedance magnitude and phase degree are most pronounced, assessing the extent to which remote converters affect the system stability seen by local converters. The influence of different converter control modes, e.g., active power/AC voltage control (PV) and active power/reactive power control (PQ), alongside varying converter parameters, on system dynamics and inter-network interactions. Utilizing a small signal impedance model the study elucidates the impact of integrating converters into networks on overall system performance.

The rest of the paper is structured as follows: Section 2 addresses converter impedance modelling, while Section 3 outlines the analysis of converter-network interactions considering a system with two converters. Sections 4 presents the simulation results and finally, conclusions are drawn in Section 5.

2. CONVERTER IMPEDANCE

In this section, the configuration of the grid-integrated Voltage Source Converter (VSC) is presented, incorporating essential components: the PLL, inner and outer control loops, alongside an integrative filtering mechanism. Each control structure is clarified, highlighting essential components, with small signal stability assessed through an impedance-based methodology. The process commences with the model's linearization, whereby the converter admittance is defined as the ratio of the converter's response current, (ΔI_o), to the voltage disturbance, (ΔV_o), as:

$$\mathbf{Y_{vscon}} = -\frac{\Delta \mathbf{I_o}}{\Delta \mathbf{V_o}} \quad (1)$$

This relationship is subsequently reformulated within the positive-negative(**pn**) frame, as [13]:

$$\mathbf{Y_{vscon}pn(s)} = \begin{bmatrix} \mathbf{Y_{vsconpp}(s)} & \mathbf{Y_{vsconpn}(s)} \\ \mathbf{Y_{vsconnp}(s-2jw_0)} & \mathbf{Y_{vsconnn}(s-2jw_0)} \end{bmatrix} \quad (2)$$

It is imperative to recognize that the impedance characteristics of converters are profoundly influenced by the inherent properties of filter components and the overarching control design strategy, highlighting the intricate symbiosis between component design and system stability.

Fig.1 illustrates the control segment of the grid-connected configuration. Detailed descriptions and tuning specifications for this design are well-understood and can be found in [13][14]. Nonetheless, a brief overview is provided herein. The PLL ensures synchronization, while AC current regulation occurs in the synchronous reference frame, facilitated by dual controllers. These controllers enhanced with suitable cross-coupling terms and voltage feed-forward strategies, operate with the outer loop controller, equippedd with either the PV or PQ controller. This discussion highlights the intricate manner in which the converter integrates with the grid, emphasizing the critical role of each parameter in the connectivity illustrated in Fig.1.

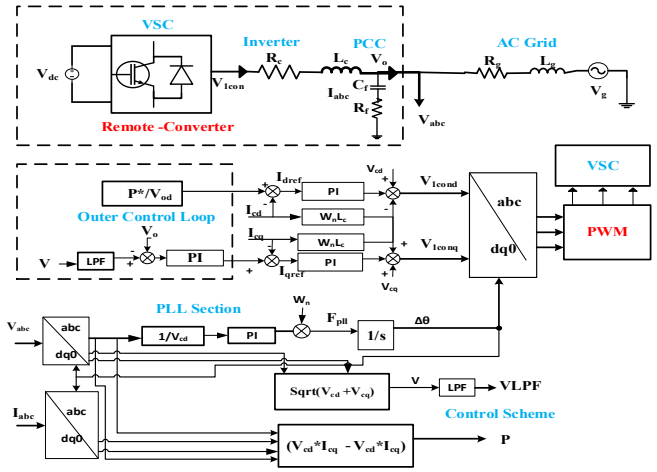

Fig. 1: schematic of a grid – connected controller structure

System stability is analysed through determining the equivalent admittances of the converter (Y_{conv}) and the grid (Z_{grid}). The frequency-domain matrix, represented as, (Y_{conv}*Z_{grid}), further aids in this assessment [14]. Using the GN diagrams derived from this matrix across steady-state operating points, the system's stability boundary can be identified.

3. MULTI-CONVERTER INTERACTION ANALYSIS

This section explores the dynamics of multi-converter interaction using impedance method analysis, based on the setup illustrated in Fig. 2.

Within this part, the impedance ratio (IR) is introduced as a key metric for evaluating converter-network dynamics. In Fig. 2, the impedance changes at the local converter terminal, i.e., before and after-connection of the remote converter can serve as significant indicators of the impact of the remote converter on the terminal conditions of the local converter. These interactions encompass both the network conditions and the behaviour of the remote converter.

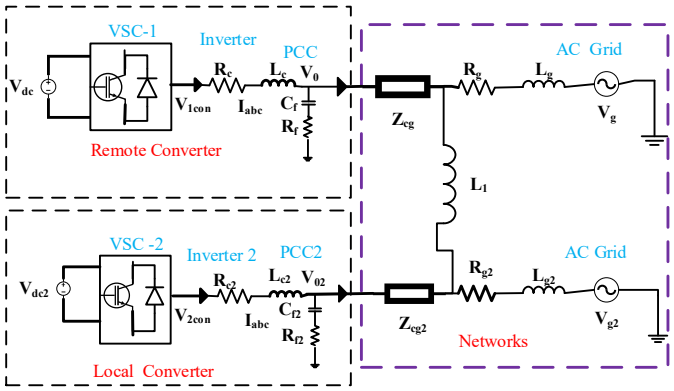

Fig. 2: multi-converter network topology

The IR, mathematically defined as the ratio of the combined impedance of the converter and network to the sole network impedance, is expressed as:

$$\mathbf{IR} = (\mathbf{Z_{(network+conv)}} / \mathbf{Z_{(network)}}) \quad (3)$$

where $Z_{network+conv}$ signifies the impedance of network seen at the local converter terminal when the remote converter is connected, while $Z_{network}$ represent the network impedance seen at the local converter terminal without the remote converter, which is related to the short circuit ratio (SCR). For the circuit shown in Fig. 2, $Z_{network}$ can be directly calculated from the impedances of the network, while $Z_{network+conv}$ can also be obtained if the impedance of the remote converter is known.

4. IMPEDANCE CHANGES OF SIMULATION RESULTS

In these sections, the proposed impedance ratio methodology is validated, enhanced by eigenvalue analysis, through time-domain and frequency-domain (FD) simulations. Time-domain simulations employed MATLAB/Simulink, while FD analysis using analytically developed converter impedance is also carried out in MATLAB. Key electrical and converter control parameters for the multi-converter system are detailed in Tables 1 and 2. The findings concentrate on two primary network scenarios between the two converters: strong network (Coupling One) and weak network (Coupling Two).

Table 1: Control Parameters for VSCs Controller

Parameters	Values
ω_n	$2*\pi*60$
Current loop PI gains: K_{pic}, K_{ic}	$Lc*\omega_n*2$, $Lc*\omega_n^2$
PLL PI gains: K_{ppll}, K_{ippll}	$2*\pi*60$, $(2*\pi*60)^2$
AC voltage controller PI gains: K_p, K_u	1.2, 6 and 1.5, 7.5 pu

Table 2: The system parameter for weak and strong Coupling

Parameter	Coupling- one	Coupling- two
R_c, R_{c2}	0.01pu, 0.01pu	0.01pu, 0.01pu
L_c, L_{c2}	0.1,0.1	0.1,0.1
L_1	0.1pu	0.3pu
R_g	0.0167	0.0167
R_{g2}	0.0167	0.0167
L_g	0.2pu	0.36pu
L_{g2}	0.22pu	0.38pu
L_{cg}	0.16pu	0.25pu
L_{cg2}	0.18pu	0.26pu
R_{cg}	0.0167pu	0.0167pu
R_{cg2}	0.0167pu	0.0167pu
SCR	3.25	1.92

4.1 Impedance simulation Results under Coupling One

Within the parameters established for Coupling One in the design of multi-converter networks, the validation of impedance under the effect of different (PV) and (PQ) outer loop control models are depicted in Fig.3 for both remote and local converters. Due to space limitation, only the positive impedance $\mathbf{Z_{vsconpp(s)}}$ is presented herein. As seen, the analytical impedances match well with those obtained from the time-domain simulation models using frequency sweeping method. Under the two different PV and PQ controls, the impedances are largely identical under above 150 Hz. However, discrepancies emerge below 150 Hz, underscoring the significant impact of the outer loop on converter impedance. Specifically, under PQ control, the magnitude of $\mathbf{Z_{vsconpp(s)}}$ between 50 and 92 Hz is smaller compared to that under PV control, thus contributing to better system stability [14].

Fig.4(a) presents a comparison between the $Z_{pp(s)}$ of the combined impedance of the remote converter and networks ($Z_{network+conv}$) and solely the networks ($Z_{network}$). As can be seen, beyond 150 Hz, the magnitude of $Z_{(network+conv)}$ evidences a diminished impedance change, signifying a positive contribution towards system stability enhancement. A specific damping effect is observed at 148 Hz, where the impedance magnitude reaches 0.9, with phase angles registering at 77 and 79 degrees under PQ and PV controls, respectively. However, a clear preference for one control method over another for stability enhancement remains undetermined.

Fig.4(b) elucidates the Impedance Ratio (IR) analysis outcomes, revealing significant alignment between the PQ and PV control models, except in the 100-170 Hz frequency range for K_{pp}. Under PQ control, an IR magnitude of 1.1 at 121 Hz and a phase of -8.6 degrees at 151 Hz are observed, modestly below PV control's IR magnitude of 1.3 at 130 Hz and a phase shift of -11 degrees at 150 Hz. This indicates that PQ control exhibits a marginally smaller phase shift compared to PV control. In this context, PV control indicates a slightly greater magnitude, indicating potential stability issues due to increased impedance magnitude.

Since the impedances are 2x2 matrixes, Fig. 5 present the eigenvalues of the IR under the two-control systems of PQ and PV. Specifically, Fig. 5(a) illustrates that the PV control's IR magnitude stands at 1.15 at 127 Hz with a phase of -11 degrees at 153 Hz, marginally greater than the PQ control's IR magnitude of 1.08 at 125 Hz and phase of -8.2 degrees at 161 Hz. This suggests higher impedance and phase angle within the frequency range of 100-190 Hz under PV control.

Fig.6 presents Nyquist plots for a system with and without a remote converter, utilizing PQ and PV control modes for the remote converter while the local converter operates in PV mode. Compared to Fig.5, the eigenvalue Impedance Ratio (IR) magnitude and phase correlate with Nyquist stability. Notably, the system exhibits similar stability with or without the remote converter under PQ control, which is superior to the stability observed with PV control. This enhanced stability is attributed to the minimal impact of the remote converter on the local converter under PQ control.

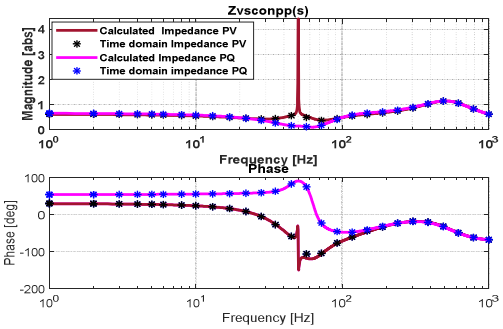

Fig. 3: Impedance of remote converter with PQ and PV Control mode

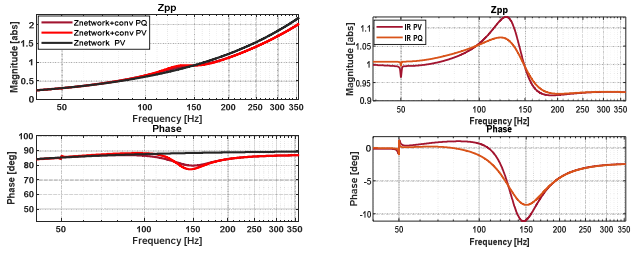

Fig.4: (a) Impedance of Znetwork v.s. Znetwork+conv and (b) IR change

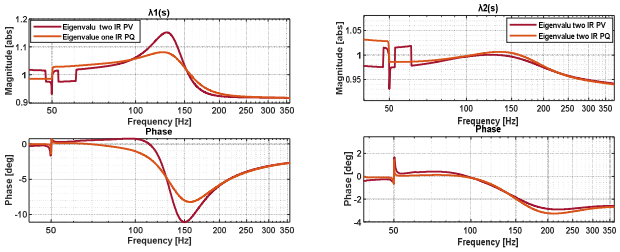

Fig.5: Eigenvalue one and two corresponding IR change

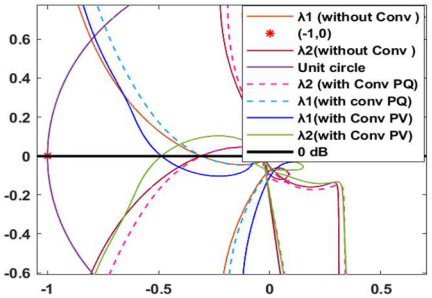

Fig. 6: Nyquist Plots Without and with Remote Converter (PV and PQ) and with Local Converter in PV Mode under coupling one parameters

4.2 Impedance simulation results under Coupling Two

Assessing the impact of the proposed method on multi-converter network dynamics under Coupling Two settings (Table 2), the positive sequence impedances $\mathbf{Z_{pp(s)}}$ are shown in Fig.7(a). Here, variations in outcomes under PQ and PV controls highlight the outer loop's influence on impedance within multi-converter networks. PQ control shows reduced magnitude $\mathbf{Z_{network+conv}}$ in the 100-120 Hz range compared to PV, indicating improved stability. In addition, PQ's enhanced damping markedly diverges from the 90º phase, signaling superior stability, in contrast to PV's phase oscillations (70º-110º) within 75-120 Hz, hinting at negative resistance and potential for instability. A distinct instability under PV is noted at 114 Hz, which is not present with PQ control. Beyond 135 Hz, both controls show similar impedance and phase, both under 90º, with PV noting a notable peak at 118 Hz indicating sharp damping.

Figs.7(b) and 8 illustrate the eigenvalues of the Impedance Ratio (IR) and the Impedance Ratio (K_{pp}), respectively. These figures reveal that under PV control of the remote converter, the impedance magnitude seen by the local converter significantly increases, whereas PQ control maintains a stable magnitude, with IR close to 1 and phase angles ranging from 0º to -15º within the 80-120 Hz range. In contrast, PV control exhibits a broader IR magnitude range (0.6 to 3) and phase shifts (-78º to 4.6º), indicating that under weak network conditions (Coupling Two), PQ control at the remote converter has a minimal impact on the stability of the local converter, while PV control can negatively affect it.

Fig.9 presents Nyquist plots for a system with and without a remote converter, using PQ and PV control modes, while the local converter operates in PV mode under Coupling Two parameters. Compared to Fig.8, the eigenvalue Impedance Ratio (IR) magnitude and phase correlate with Nyquist stability. The system remains stable under PQ control, even exceeding the stability of the system without the remote converter, while PV control leads to instability, linked to negative resistance, as shown in Fig.7a.

Figs.7-8 indicate that shifts in negative resistance, changes in IR, and eigenvalues under PV control between 80-120 Hz led to instability for the local converter, corroborated by the Nyquist plots in Fig.9. The oscillation frequency under PV control is around 114 Hz. Fig.10's time-domain simulation confirms these findings, showing system instability at a PLL frequency of 30 Hz, with oscillation frequency aligning with Nyquist analysis. At t = 9.2 s, the PLL bandwidth adjustment from 10 Hz to 30 Hz further validates this instability.

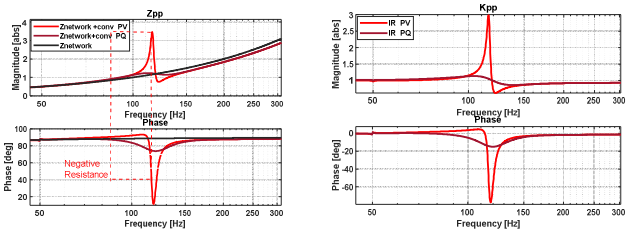

(a) (b)

Fig.7(a): Impedance comparison between Znetwork+conv and Znetwork,; (b) Impedance Ratio IR (represented with K_{pp})

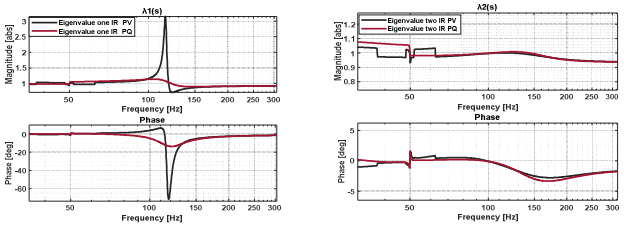

(a) (b)

Fig. 8: Eigenvalue of the impedance ratio (IR) change

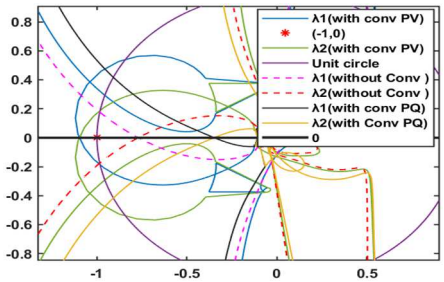

Fig.9: Nyquist Plots Without and with Remote Converter (PV and PQ) and with Local Converter in PV Mode under coupling two parameters

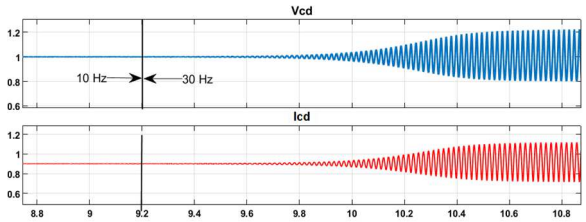

Fig.10: Time domain simulation of local converter d-axis voltage and current Under Coupling Two (when the PLL control parameters is changed).

Fig.11 presents Nyquist plots illustrating system stability with a remote converter under PQ control and without the converter, while the local converter operates in PV mode. This analysis examines the impact of the remote converter's network interaction on the local converter. Fig.12 supports these findings through time-domain simulations of power variation in the local converter. The assessment reveals that a remote converter with PQ control enhances stability compared to a system without a remote converter. Time-domain simulations explore configurations of P1=0.9 and variable P2 ranging from 0.9 to 1.4. Notably, at the 8.4 and 8.6-second intervals, adjustments in P2 to 1.4 (with a converter, Fig. 12a) and to 1.2 (without a converter, Fig. 12b) induce significant oscillations or overshoot, indicating instability. Modifications to VSC-1's size further compromise stability. Additional analysis is required to understand multi-converter network interactions under weak grid coupling.

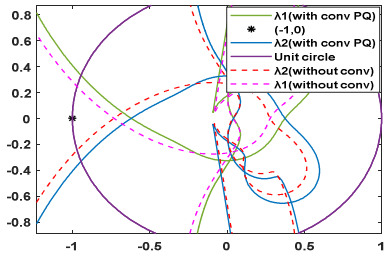

Fig.11:Nyquist Plots without and with remot converter of PQ

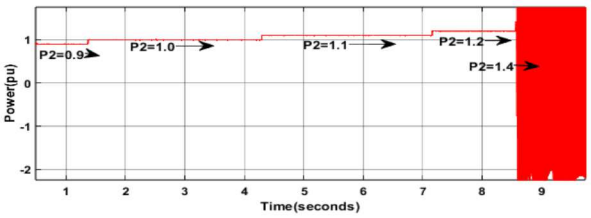

(a)

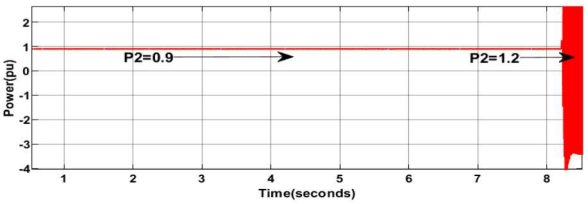

(b)

Fig.12 Time domain simulations under varying power levels, (a): with remote converter under PQ control; and (b): without remote converter

In summary, the Impedance Ratio (IR) serves as an indicator of the network impedance perceived by the local converter, both with and without the presence of the remote converter. An IR magnitude exceeding 1 indicates an increase in the effective impedance seen by the local converter, while a positive angle (>0) suggests reduced damping, leading to an increase in the inductive angle. This scenario can significantly impact network interactions, potentially inducing resonance or instability, as evidenced in Fig. 7a. Conversely, an IR magnitude equal to or less than 1 signifies a reduction in the effective impedance perceived by the local converter, accompanied by a negative angle (<0), indicating increased damping. This results in a decrease in the inductive angle or reduced influence on network interactions, as illustrated in Fig. 4b.

5. CONCLUSION

This paper presented a detailed investigation into impedance change and system stability in multi-converter configuration, employing an impedance-based methodology underscored by impedance ratio and eigenvalue analysis. It systematically examines the interactions between remote converter and network components under different control modes, e.g., (PV and PQ) as well as different control parameters setting. The analysis identifies the critical frequencies where the potential instability arises from the interaction between converter control strategies and network characteristics, categorizing impedance behaviour into high IR (indicating high interaction), and low IR value equal (indicating low interaction value). Overall, the findings highlight how high impedance magnitude changes and phase angle variations exacerbate interactions, impacting system stability seen by the local converter. Significantly, the impedance framework reveals the crucial role of converter interplay, notably emphasizing the stability benefits of PQ control mode over PV, as well as the stability enhancement conferred by integrating the remote converter with PQ control into the network. The research also opens avenues for potential network simplification, meriting further investigation.

REFERENCE

[1] Yoon, C., Wang, X., Bak, C. L., & Blaabjerg, F. (2015). Stabilization of multiple unstable modes for small-scale inverter-based power systems with impedance-based stability analysis. Conference Proceedings - IEEE Applied Power Electronics Conference and Exposition - APEC, 2015-May (May), 1202–1208. https://doi.org/10.1109/APEC.2015.7104500

[2] Power Sources Manufacturers Association, IEEE Power Electronics Society, Annual IEEE Computer Conference, IEEE Industry Applications Conference, Annual IEEE Applied Power Electronics Conference and Exposition 30 2015.03.15-19 Charlotte, N., & APEC 30 2015.03.15-19 Charlotte, N. (n.d.). IEEE Applied Power Electronics Conference and Exposition (APEC), 2015 15-19 March 2015, Charlotte Convention Center, Charlotte, North Carolina

[3] Henderson, C., Egea-Alvarez, A., Kneuppel, T., Yang, G., & Xu, L. (2024). Grid Strength Impedance Metric: An Alternative to SCR for Evaluating System Strength in Converter Dominated Systems. IEEE Transactions on Power Delivery, 39(1), 386–396. https://doi.org/10.1109/TPWRD.2022.3233455

[4] Wen, B., Dong, D., Boroyevich, D., Burgos, R., Mattavelli, P., & Shen, Z. (2016). Impedance-based analysis of grid-synchronization stability for three-phase paralleled converters. IEEE Transactions on Power Electronics, 31(1), 26–38. https://doi.org/10.1109/TPEL.2015.2419712

[5] Chen, Y., Xu, L., Egea-Alvarez, A., Marshall, B., Rahman, M. H., & Oluwole, A. D. (2021). MMC Impedance Modeling and Interaction of Converters in Close Proximity. IEEE Journal of Emerging and Selected Topics in Power Electronics, 9(6), 7223–7236. https://doi.org/10.1109/JESTPE.2020.3031489

[6] Dong, D., Wen, B., Boroyevich, D., Mattavelli, P., & Xue, Y. (2015). Analysis of phase-locked loop low-frequency stability in three-phase grid-connected power converters considering impedance interactions. IEEE Transactions on Industrial Electronics, 62(1), 310–321. https://doi.org/10.1109/TIE.2014.2334665

[7] He, J., Li, Y. W., Bosnjak, D., & Harris, B. (2013). Investigation and active damping of multiple resonances in a parallel-inverter-based microgrid. IEEE Transactions on Power Electronics, 28(1), 234–246. https://doi.org/10.1109/TPEL.2012.2195032

[8] Wang, Y., Wang, X., Blaabjerg, F., & Chen, Z. (2017). Harmonic instability assessment using state-space modeling and participation analysis in inverter-fed power systems. IEEE Transactions on Industrial Electronics, 64(1), 806–816. https://doi.org/10.1109/TIE.2016.2588458

[9] Liao, Y., & Wang, X. (2020). Impedance-Based Stability Analysis for Interconnected Converter Systems with Open-Loop RHP Poles. IEEE Transactions on Power Electronics, 35(4), 4388–4397. https://doi.org/10.1109/TPEL.2019.2939636

[10] Xiao, Q., Mattavelli, P., Khodamoradi, A., & Tang, F. (2019). Analysis of Transforming dq Impedances of Different Converters to A Common Reference Frame in Complex Converter Networks. CES Transactions on Electrical Machines and Systems, 3(4), 342–350. https://doi.org/10.30941/CESTEMS.2019.00046.

[11] Zhang, C., Molinas, M., Rygg, A., & Cai, X. (2020). Impedance-Based Analysis of Interconnected Power Electronics Systems: Impedance Network Modeling and Comparative Studies of Stability Criteria. IEEE Journal of Emerging and Selected Topics in Power Electronics, 8(3), 2520–2533. https://doi.org/10.1109/JESTPE.2019.2914560

[12] Cao, W., Ma, Y., & Wang, F. (2017). Sequence-Impedance-Based Harmonic Stability Analysis and Controller Parameter Design of Three-Phase Inverter-Based Multibus AC Power Systems. IEEE Transactions on Power Electronics, 32(10), 7674–7693. https://doi.org/10.1109/TPEL.2016.2637883

[13] Huang, L., Wu, C., Zhou, D., & Blaabjerg, F. (2022). A Double-PLLs-Based Impedance Reshaping Method for Extending Stability Range of Grid-Following Inverter under Weak Grid. *IEEE Transactions on Power Electronics*, *37*(4), 4091–4104. https://doi.org/10.1109/TPEL.2021.3127644

[14] Sun, J. (2011). Impedance-based stability criterion for grid-connected inverters. IEEE Transactions on Power Electronics, 26(11), 307